

Organized Grouped Discrete Representation for Object-Centric Learning

Rongzhen Zhao, Vivienne Wang, Juho Kannala, Joni Pajarinen

Aalto University, Espoo 02150, Finland
{rongzhen.zhao, vivienne.wang, juho.kannala, joni.pajarinen}@aalto.fi

Abstract

Object-Centric Learning (OCL) represents dense image or video pixels as sparse object features. Representative methods utilize discrete representation composed of Variational Autoencoder (VAE) template features to suppress pixel-level information redundancy and guide object-level feature aggregation. The most recent advancement, Grouped Discrete Representation (GDR), further decomposes these template features into attributes. However, its naive channel grouping as decomposition may erroneously group channels belonging to different attributes together and discretize them as sub-optimal template attributes, which losses information and harms expressivity. We propose *Organized GDR* (OGDR) to organize channels belonging to the same attributes together for correct decomposition from features into attributes. In unsupervised segmentation experiments, OGDR is fully superior to GDR in augmentating classical transformer-based OCL methods; it even improves state-of-the-art diffusion-based ones. Codebook PCA and representation similarity analyses show that compared with GDR, our OGDR eliminates redundancy and preserves information better for guiding object representation learning. The source code is available in the supplementary material.

Introduction

Under self or weak supervision, Object Centric Learning (OCL) (Greff et al. 2019; Burgess et al. 2019) can represent dense image or video pixels as sparse object feature vectors, with corresponding segmentation masks as byproducts that reflect how well the object features are. This is meta-physically bio-plausible, because we humans perceive visual scenes as objects for higher-level vision cognition, like understanding, reasoning, planning, and decision-making (Bar 2004; Cavanagh 2011; Palmeri and Gauthier 2004). This is also physically desired, because object-level representation of images or videos is more versatile for visual tasks involving different modalities (Yi et al. 2020; Wu et al. 2023a).

Representative OCL includes the ones that are mixture-based (Locatello et al. 2020; Kipf et al. 2022), transformer-based (Singh, Deng, and Ahn 2022; Singh, Wu, and Ahn 2022), foundation-based (Seitzer et al. 2023; Zadaianchuk, Seitzer, and Martius 2024) and diffusion-based (Wu et al.

2023b; Jiang et al. 2023). The latter three all utilize intermediate representation to suppress inter-pixel dissimilarities and enhance intra-object similarities so as to guide object-level feature aggregation. For the transformer and diffusion-based ones, such guidance is obtained by representing images or videos with template features from a pretrained Variational Autoencoder (VAE) (Singh, Deng, and Ahn 2022; Van Den Oord, Vinyals, and Kavukcuoglu 2017) codebook. Such codes are in limited number and shared across the dataset. The most recent work GDR (Zhao et al. 2024) further decomposes those template features into more reusable attributes. This suppresses inter-pixel dissimilarity and enhances intra-object similarity more, achieving better performance and generalization on transformer-based baselines.

However, GDR’s *naive channel grouping* on intermediate representation *as the decomposition* from features to attributes, neglects the fact that channels belonging to the same attribute may scatter among all channel places rather than together in one adjacent channel group. In other words, **as shown in Fig. 1**, channels belonging to different attributes are grouped together and discretized into sub-optimal template attributes, which loses information and damages model expressivity. Besides, GDR only works on transformer-based methods, not diffusion-based ones.

We propose (i) *Organized Grouped Discrete Representation* (OGDR), which organizes intermediate representation channels for grouped discretization, overcoming the information loss and model expressivity damage. (ii) OGDR is applicable not only to classical transformer-based methods, but also to state-of-the-art diffusion-based ones. (iii) Comprehensive experiments demonstrate how well OGDR improves the baselines. (iv) Intuitive analyses illustrate statistically and visually how OGDR channel organizing augments model expressivity and guides object representation learning. (v) Ablation studies show how to configure the hyperparameters and maximize OGDR’s effectiveness.

Related Work

Object Centric Learning (OCL). Mainstream OCL utilizes SlotAttention (Locatello et al. 2020; Bahdanau, Cho, and Bengio 2015) to aggregate dense feature maps into sparse object features, and further utilizes intermediate representation, which suppresses pixel-level redundant details, to handle textured objects. Transformer-based OCL, like SLATE

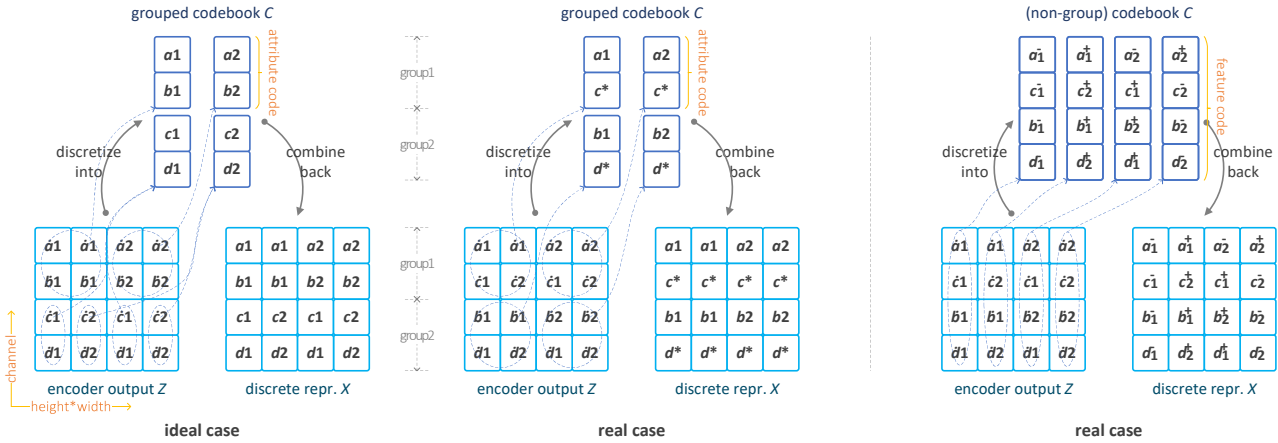


Figure 1: Problem. Naive grouped discretization loses information (*left*) while non-grouped discretization retains redundancy (*right*). Suppose a dataset can be fully represented by four template features, which can be decomposed into two attribute groups, each with two fundamental template attributes: $(a_1, b_1)^T$ and $(a_2, b_2)^T$, $(c_1, d_1)^T$ and $(c_2, d_2)^T$; Channels a and b form one attribute, c and d another; Arbitrary continuous values $\hat{a}_1, \hat{a}_2, \dots, \hat{d}_2$ should be ideally discretized into a_1, a_2, \dots, d_2 , respectively. In the **grouped ideal case**, for Z of channel order a - b - c - d , direct two-grouping puts channels belong to the same attribute together. Thus continuous attribute $(\hat{a}_1, \hat{b}_1)^T$ can be discretized into template attribute $(a_1, b_1)^T$, and so do the others. The resulting grouped discrete representation X ideally represents Z . In a **grouped real case**, for Z of channel order a - c - b - d , naive grouping puts channels a and c together, which belong to different attributes. Thus continuous attributes $(\hat{a}_1, \hat{c}_1)^T$ and $(\hat{a}_1, \hat{c}_2)^T$ are discretized into (a_1, c_*) , where c_* is the mean of c_1 and c_2 . The resulting X loses some information of Z and damages model expressivity. In all **non-grouped real cases**, regardless of the channel order, every continuous feature in Z , e.g., $(\hat{a}_1, \hat{c}_1, \hat{b}_1, \hat{d}_1)$ is discretized into a template feature in C , e.g., $(a_1^-, c_1^-, b_1^-, d_1^-)^T$, where a_1^- is some smaller value of a_1 . The resulting non-grouped discrete representation X does not lose information of Z but leaves over too much redundancy.

(Singh, Deng, and Ahn 2022) and STEVE (Singh, Wu, and Ahn 2022), generates input tokens from slots via a transformer decoder (Vaswani et al. 2017), guided by dVAE (Singh, Deng, and Ahn 2022) discrete representation (Fig. 2 first row left); Diffusion-based OCL, like SlotDiffusion (Wu et al. 2023b) and LSD (Jiang et al. 2023), recovers input noise from slots via a diffusion model (Rombach et al. 2022), guided by VQ-VAE (Van Den Oord, Vinyals, and Kavukcuoglu 2017) discrete representation (Fig. 2 first row right); Foundation-based OCL, like DINOSAUR (Seitzer et al. 2023) and VideoSAUR (Zadaianchuk, Seitzer, and Martius 2024), reconstructs input features from slots via a spatial broadcast decoder (Watters et al. 2019), guided by well-pretrained features of the foundation model DINO (Caron et al. 2021; Oquab et al. 2023). We focus on VAE part of transformer- and diffusion-based methods.

Variational Autoencoder (VAE). dVAE (Singh, Deng, and Ahn 2022) is adopted in classical transformer-based OCL (Singh, Deng, and Ahn 2022; Singh, Wu, and Ahn 2022), to discretize intermediate representation of its encoder output by selecting template features in a codebook with hard Gumbel sampling (Jang, Gu, and Poole 2017) (Fig. 2 second row left). VQ-VAE (Van Den Oord, Vinyals, and Kavukcuoglu 2017) is employed in state-of-the-art diffusion-based OCL (Jiang et al. 2023; Wu et al. 2023b), to discretize intermediate representation by replacing features with the most similar codebook codes (Fig. 2 second row right). Techniques of other VAE variants, like grouping (Yang et al. 2023), residual (Barnes, Rizvi, and

Nasrabadi 1996) and clustering (Lim, Jiang, and Yi 2020), are also worth exploiting for better discrete intermediate representation to guide object-centric representation learning. We borrow some ideas from them.

Channel Grouping. Splitting features along the channel dimension and transforming them separately is often used to promote representation diversity (Krizhevsky, Sutskever, and Hinton 2012; Chen et al. 2019; Huang et al. 2018; Zhao, Wu, and Zhang 2021; Zhao, Li, and Wu 2022). This is also explored in OCL. SysBinder (Singh, Kim, and Ahn 2022) groups slot queries into different “blocks” to aggregate different attributes of objects, yielding more interpretability in object representation but limited performance boosts. The most recent OCL augmentor GDR (Zhao et al. 2024) groups the VAE discrete representation into combinatorial template attributes, to guide object feature aggregation in transformer-based methods (Fig. 2 second row center). It augments baselines in both performance and generalization, but its naive channel grouping as decomposition somehow harms model expressivity. Our OGDR is more beneficial to both transformer- and diffusion-based methods.

Proposed Method

We propose *Organized* Grouped Discrete Representation (OGDR), a general augmentor to representative OCL methods like the transformer-based (Singh, Deng, and Ahn 2022; Singh, Wu, and Ahn 2022) and the diffusion-based (Wu et al. 2023b; Jiang et al. 2023).

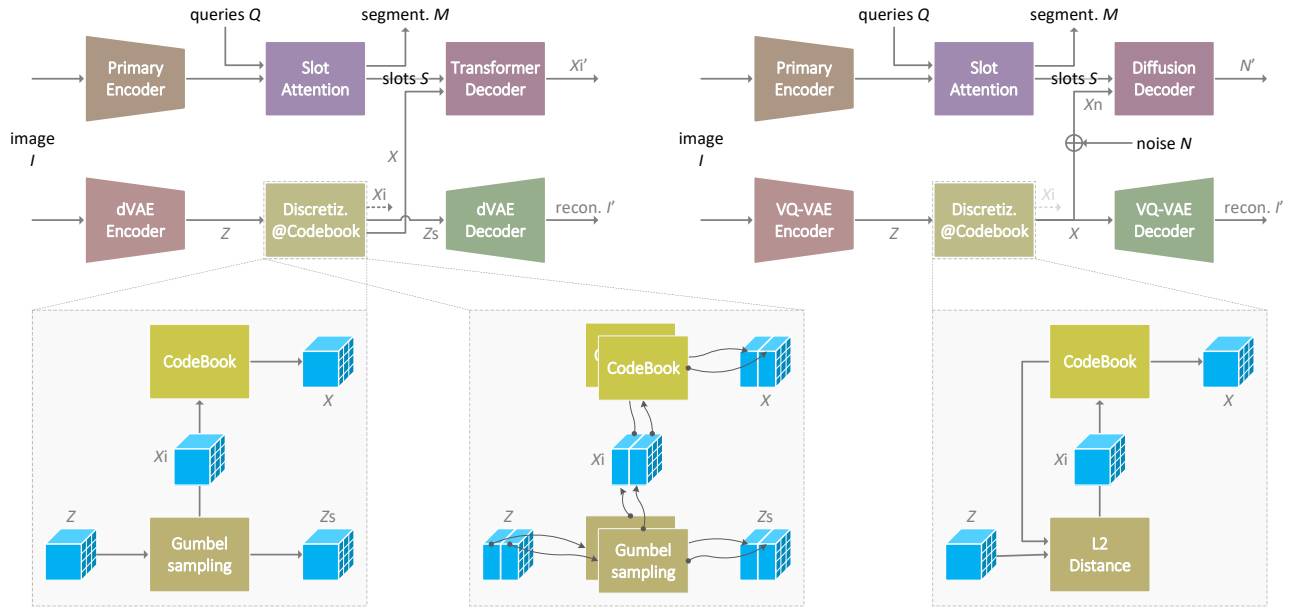


Figure 2: Preliminary. First row: model architectures of transformer-based OCL (left) and diffusion-based OCL (right). Second row: non-grouped intermediate representation discretization in dVAE (left), grouped discrete representation in dVAE (GDR) (center), and non-grouped discretization in VQ-VAE (right). GDR can be extended to VQ-VAE.

Notations: image or video frame I , continuous representation Z , discrete representation X , and noise N are tensors in shape (height, width, channel); queries Q and slots S are tensors in shape (number, channel); segmentation M is a tensor in shape (height, width).

Preliminary: Discrete Representation

Both transformer-based classics and diffusion-based state-of-the-arts learn to extract object features (slots) from images or videos, guided by their discrete representation.

Transformer-based architecture is drawn in Fig. 2 first row left. Input image or video frame I is encoded by a primary encoder and aggregated by SlotAttention (Locatello et al. 2020) into slots S under queries Q , with objects (and the background) segmentation masks M as byproducts. Meanwhile, a pretrained VAE model represents I as discrete X and the corresponding code indexes X_i . Afterwards, with a transformer decoder, S is challenged to reconstruct X_i as classification guided by causally masked X . For video modality, current slots S is transformed by a transformer encoder block into queries for next frame.

Specifically, discrete representation for transformer-based OCL is obtained as in Fig. 2 second row left:

(i) predefine a codebook C holding n c -dimensional learnable codes as template features; (ii) transform input I with dVAE encoder into continuous intermediate representation Z ; (iii) sample Z via Gumbel and yield one-hot indexes X_i , with soft sampling Z_s for dVAE decoding; (iv) index template features from C by X_i and compose the discrete representation X .

Diffusion-based architecture is drawn in Fig. 2 first row right. The only difference is that with a conditional diffu-

sion model decoder, S is challenged to reconstruct Gaussian noise N being added as regression, guided by X .

Specifically, discrete representation for diffusion-based OCL is obtained as in Fig. 2 second row right:

(i) predefine a codebook C holding n learnable codes as template features; (ii) transform input I with VQ-VAE encoder into continuous intermediate representation Z ; (iii) find the most similar code indexes X_i in C for every superpixel in Z by least L2 distance; (iv) select template features in C by X_i to form discrete representation X , which is also for VQ-VAE decoding.

The **guidance** here means that with X as cues and S as conditions, a transformer or diffusion decoder strives to reconstruct I , which forces S to extract as much object information as possible. The key is suppressing texture noises with X and enhancing object feature consistency.

Naive Grouped Discrete Representation

GDR or Grouped Discrete Representation (Zhao et al. 2024) is based on dVAE and only works for transformer-based OCL. Its naive channel grouping as decomposition from features to attributes enhances the aforementioned guidance but harms model expressivity.

Similar to Fig. 2 second row center, we unify the VAE part of both transformer-based and diffusion-based methods with VQ-VAE, and transfer such naive GDR technique to VQ-VAE. This yields a general OCL augmentor because after pretraining, VQ-VAE provides the already learnt discrete representation required by the diffusion.

Beforehand, suppose a dataset is fully described by n c -dimensional template features that are fully described by g attribute groups, each of which has a d -dimensional tem-

Figure 3: Solution. Organized grouped discrete representation (OGDR) is obtained by (i) projecting Z up in channel dimension with pseudo-inverse of matrix W ; (ii) conducting naive channel grouping and discretization by L2 distance upon attribute codes from Z_+ into X_+ and code indexes X_i ; (iii) adding residual Z_+ to X_+ for pretraining only; (iv) projecting X_+ down in channel dimension with learnable matrix W into X ; and (v) normalizing X finally.

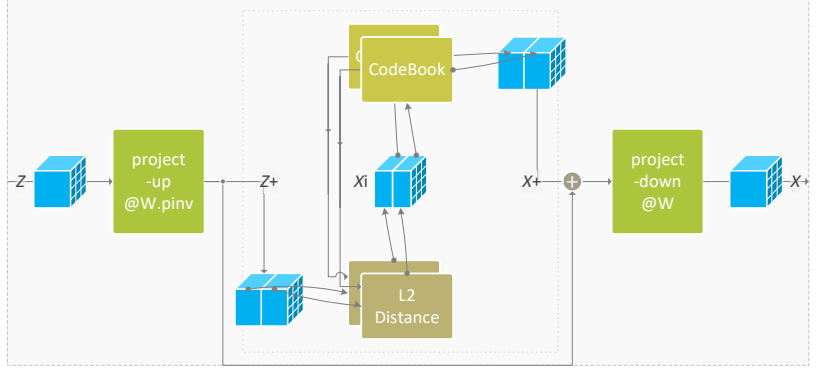


plate attributes. Here $n == a^g$ and $c == g \times d$. Accordingly, we predefine a set of attribute codebooks $C = \{C^{(1)}, C^{(2)} \dots C^{(g)}\}$, whose codes parameters are in shape (g, a, d) . Ideally, the combinations of those attribute-level codebooks are equivalent to the non-grouped feature-level codebook, whose code parameters are in shape (n, d) .

This is the same for both dVAE and VQ-VAE.

Afterwards, we transform input I with VAE encoder into continuous intermediate representation Z .

For grouped discretization, in dVAE, GDR samples Z via Gumbel noise (Jang, Gu, and Poole 2017) and yields tuple code indexes X_i , along with soft sampling Z_s :

$$Z_s = \text{softmax}\left(\frac{Z^{(1)} + G}{\tau}\right) \parallel \text{softmax}\left(\frac{Z^{(2)} + G}{\tau}\right) \parallel \dots \parallel \text{softmax}\left(\frac{Z^{(g)} + G}{\tau}\right) \quad (1)$$

$$X_i = \text{argmax}(Z_s^{(1)}) \parallel \text{argmax}(Z_s^{(2)}) \parallel \dots \parallel \text{argmax}(Z_s^{(g)}) \quad (2)$$

where $Z^{(1)} \dots Z^{(g)}$ are channel groups of Z ; noise $G \sim \text{Gumbel}(\mu = 0, \beta = 1)$, with temperature τ ; \parallel is channel concatenation; $\text{argmax}(\cdot)$ is along the channel dimension.

But in VQ-VAE, we sample distances between Z and C via Gumbel noise and yield tuple code indexes X_i :

$$D = \text{l2}(Z^{(1)}, C^{(1)}) \parallel \text{l2}(Z^{(2)}, C^{(2)}) \parallel \dots \parallel \text{l2}(Z^{(g)}, C^{(g)}) \quad (3)$$

$$D_s = \text{softmax}\left(\frac{D^{(1)} + G}{\tau}\right) \parallel \text{softmax}\left(\frac{D^{(2)} + G}{\tau}\right) \parallel \dots \parallel \text{softmax}\left(\frac{D^{(g)} + G}{\tau}\right) \quad (4)$$

$$X_i = \text{argmin}(D_s^{(1)}) \parallel \text{argmin}(D_s^{(2)}) \parallel \dots \parallel \text{argmin}(D_s^{(g)}) \quad (5)$$

where $\text{l2}(\cdot, \cdot)$ means L2 distances between every vector pair in its two arguments; D_s is soft Gumbel sampling of distances D between continuous representations and codes; $\text{argmax}(\cdot)$ is along the code dimension.

Subsequently, index template attributes by X_i from C and form grouped discrete representation X ; transform X_i from tuple into scalar format:

$$X = \text{index}(C^{(1)}, X_i^{(1)}) \parallel \text{index}(C^{(2)}, X_i^{(2)}) \parallel \dots \parallel \text{index}(C^{(g)}, X_i^{(g)}) \quad (6)$$

$$X_i := a^0 \times X_i^{(1)} + a^1 \times X_i^{(2)} + \dots + a^{(g-1)} \times X_i^{(g)} \quad (7)$$

where $X_i^{(1)} \dots X_i^{(g)}$ are channel groups of X_i ; and $\text{index}(\cdot, \cdot)$ selects codes from a codebook by indexes.

This is the same for both dVAE and VQ-VAE.

Finally, as for pretraining supervision, we also add the utilization loss proposed in GDR to the VQ-VAE setting. The number of groups and corresponding codebook parameters are similar to those of GDR.

However, information loss and model expressivity damage caused by the naive channel grouping as decomposition, as shown in Fig. 1, remain unaddressed.

Organized Grouped Discrete Representation

As shown in Fig. 3, we propose organized grouping to replace the naive channel grouping of GDR. The key idea is: use a invertible projection to organize channels of the continuous intermediate representation for better grouped discretization with less information loss; then use this projection to recover the (discrete) intermediate representation. In return, less information loss leads to better model expressivity, and ultimately better OCL guidance.

Firstly, we project the intermediate representation Z up to higher channel dimension with the pseudo-inverse of a learnable matrix W :

$$Z_+ = Z \cdot \text{pinv}(W) \quad (8)$$

where Z is in shape (height, width, channel= c); $\text{pinv}(\cdot)$ is the pseudo-inverse operation; and matrix $\text{pinv}(W)$ is in shape (channel= c , expanded channel= $8c$).

This facilitates channels belonging to the same attributes to be placed together (i) by allowing channel reordering through such transformation and (ii) by producing more channel replicas to counteract mis-grouping.

Secondly, group the expanded representation Z_+ along the channel dimension and discretize it by L2 distance upon the attribute-level codebooks C . Accordingly, we get code indexes X_i and the expanded discrete representation X_+ . This is already formaluted above in Eq. 3-7, with only different notations of Z vs Z_+ and X vs X_+ .

Meanwhile, add Z_+ to X_+ :

$$X_+ := Z_+ \times \alpha + X_+ \times (1 - \alpha) \quad (9)$$

where α is decayed by cosine annealing¹ from 0.5 to 0 in

¹https://pytorch.org/docs/stable/generated/torch.optim.lr_scheduler.CosineAnnealingLR.html

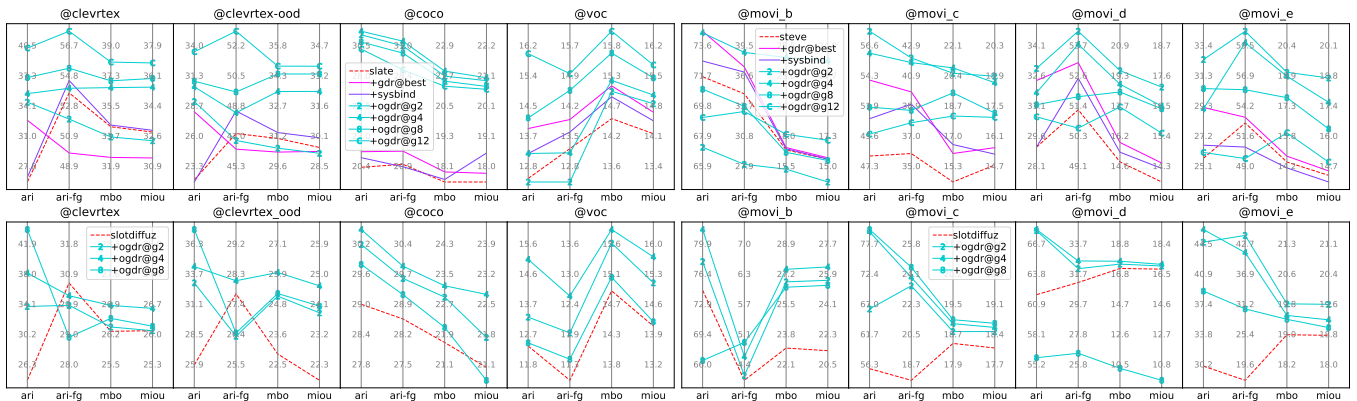


Figure 4: **OGDR** boosts both transformer-based (*top*) and diffusion-based (*bottom*) methods in OCL performance measured by unsupervised segmentation on images (*left*) or videos (*right*). The primary encoder is unified as a four-layer naive CNN. Titles are datasets; x ticks are metrics while y ticks are metric values in adaptive scope; *g2/4/8/12* are OGDR groups numbers.

the former half pretraining, and is fixed to 0 after training.

With such residual preserving information from continuous to discrete, the whole VAE can be pretrained sufficiently even if bad grouped discretization loses information.

Thirdly, project the expanded discrete representation X_+ down and yield the final organized grouped discrete representation X , as a recovery of Z :

$$X = X_+ \cdot W \quad (10)$$

where W is the aforementioned learnable matrix in shape (expanded channel= $8c$, channel= c).

Such parameter-sharing project-up and project-down enforce strong inductive bias on the organizing. Specified parameters as project-up worsens the performance.

Finally, in case of numerical instability due to matrix multiplication of pseudo-inverse, we normalize X :

$$X := \frac{X - \mathbb{E}[X]}{\sqrt{\mathbb{V}[X] + \epsilon}} \quad (11)$$

where \mathbb{E} and \mathbb{V} are mean and variance over height, width and channel; ϵ is a small number to avoid zero-division.

Hyper-parameter setting. We use typical codebook size $n=4096$, and typical channel dimension $c=256$ for transformer-based methods while $c=4$ for diffusion-based methods. Similar to GDR, group numbers can be $g2, 4, 8$ and 12 ; channel expansion rate is by default set to $8c$. Same as GDR, the corresponding available parameters are still much less than the non-grouped codebook, as grouping itself saves many times of parameters in codebook, which leaves budget for our project-up and project-down design.

Experiments

We evaluate these points with our experiments: (*i*) OGDR beats GDR and augments both transformer-based and diffusion-based OCL; (*ii*) OGDR improves OCL model expressivity while enhancing OCL guidance; (*iii*) Components of OGDR contribute to its success and how to set them.

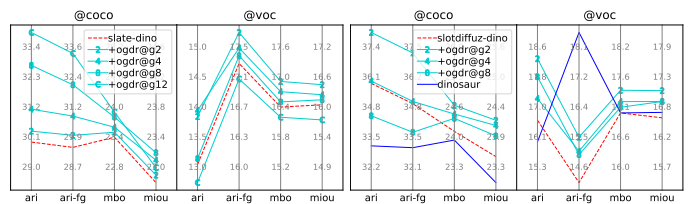


Figure 5: **OGDR** still improves both transformer-based (left) and diffusion-based (right) methods even with the foundational model DINO as the strong primary encoder.

OCL Performance

We cover the following recognized cases to evaluate object-centric learning performance with 3 random seeds.

The transformer-based models are SLATE (Singh, Deng, and Ahn 2022) for image and STEVE (Singh, Wu, and Ahn 2022) for video; the diffusion-based models are SlotDiffusion (Wu et al. 2023b) for image and its temporal variant for video. Our competitors, SysBinder (Singh, Kim, and Ahn 2022) @*g4* and GDR (Zhao et al. 2024) @*best*, are reported. DINOSAUR (Seitzer et al. 2023), the foundation-based, is also included as a reference. Naive CNN (Kipf et al. 2022; Elsayed et al. 2022) is used as a unified primary encoder.

The datasets are ClevrTex², COCO³ and VOC⁴ for image OCL, and MOVi-B/C/D/E⁵ for video OCL. They cover both synthetic and real-world cases, and each scene contains multiple objects with textures of different difficulty levels. Data processing follows the conventions.

The metrics are Adjusted Rand Index (ARI)⁶, ARI_{fg}

²<https://www.robots.ox.ac.uk/~vgg/data/clevrtex>

³<https://cocodataset.org/#panoptic-2020>

⁴<http://host.robots.ox.ac.uk/pascal/VOC>

⁵<https://github.com/google-research/kubric/tree/main/challenge/s/movi>

⁶https://scikit-learn.org/stable/modules/generated/sklearn.metrics.adjusted_rand_score.html

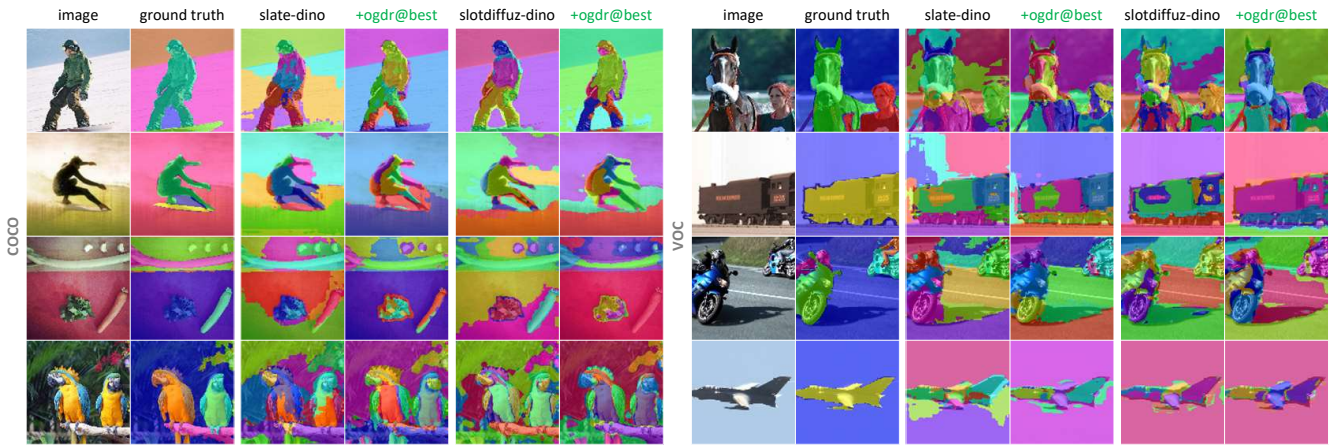


Figure 6: Qualitative results of SLATE-DINO and SlotDiffusion-DINO plus OGDR on COCO (left) and VOC (right).

(ARI foreground), mean Best Overlap (mBO) ⁷ and mean Intersection-over-Union (mIoU) ⁸ of the accuracy of the byproduct unsupervised segmentation, as the measurement of object-centric representation learning quality.

Results are shown in Fig. 4. In most cases of synthetic or real-world images or videos, our OGDR boosts OCL performance of both transformer-based classics (SLATE and STEVE) and diffusion-based state-of-the-arts (SlotDiffusion) significantly, while GDR is only applicable to the transformer-based. Upon SLATE and STEVE, OGDR beats the competitive augmentors, SysBinder and GDR, by a large margin on all datasets except MOVi-B.

We also evaluate OGDR upon these models with foundation model DINO (Caron et al. 2021) as strong primary encoder, along with DINOSAUR, as shown in Fig. 5 and 6. On either SLATE or SlotDiffusion, OGDR still boosts their OCL performance under all metrics in most cases. Particularly, OGDR even makes the old SLATE as competitive as the advanced SlotDiffusion on COCO.

Model Expressivity

We argue that our OGDR preserves information when suppressing redundancy, namely, yielding better model expressivity than GDR. This can be measured (i) by template features diversity in VAE codebook and (ii) by object separability in VAE discrete representation.

As shown in Fig. 7, OGDR codebook diversity is significantly higher than that of GDR, by counting the mean of PCA (Principal Component Analysis) ⁹ eigen-values of VAE codebook. Our organizing technique promotes the VAE model to grasp more diverse template features for better representation discretization. As shown in Fig. 8, OGDR object separability is obviously clearer than that of GDR, by

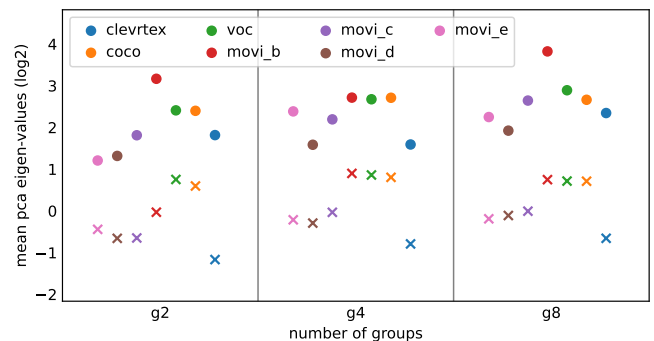


Figure 7: VAE codebook diversity measured by PCA eigen-values mean (y axis) of template features in codebook. Circles are results of our OGDR and crosses are GDR; different colors mean different datasets; the higher the better.

coloring superpixels according to their cosine similarities ¹⁰. Our organizing technique fosters better guiding representation for object representation learning.

More **interpretable** visualizations about channel organizing and discrete representation are provided in the appendix.

Ablation

The effects of designs in OGDR are listed in Fig. 1. We use the VAE pretraining performance, measured in reconstruction MSE, as the metrics for easy comparison.

Number of groups formulated in Eq. 3⁷: $g=2, 4, 8$ or 12 . As already drawn in Eq. 4 and 5, the best g is dependent on specific datasets, yet $g12$ is more likely to have lower performance than the baselines.

Channel expansion rate of the project-up formulated in Eq. 8: $c, 2c, 4c$ or $8c$. For transformer-based methods, although $8c$ usually works the best, the expansion rate for OGDR has little impact on the performance. This implies that our organizing truly works, making higher channel ex-

⁷<https://ieeexplore.ieee.org/document/7423791>

⁸https://scikit-learn.org/stable/modules/generated/sklearn.metrics.jaccard_score.html

⁹<https://scikit-learn.org/stable/modules/generated/sklearn.decomposition.PCA.html>

¹⁰https://scikit-learn.org/stable/modules/generated/sklearn.metrics.pairwise.cosine_similarity.html

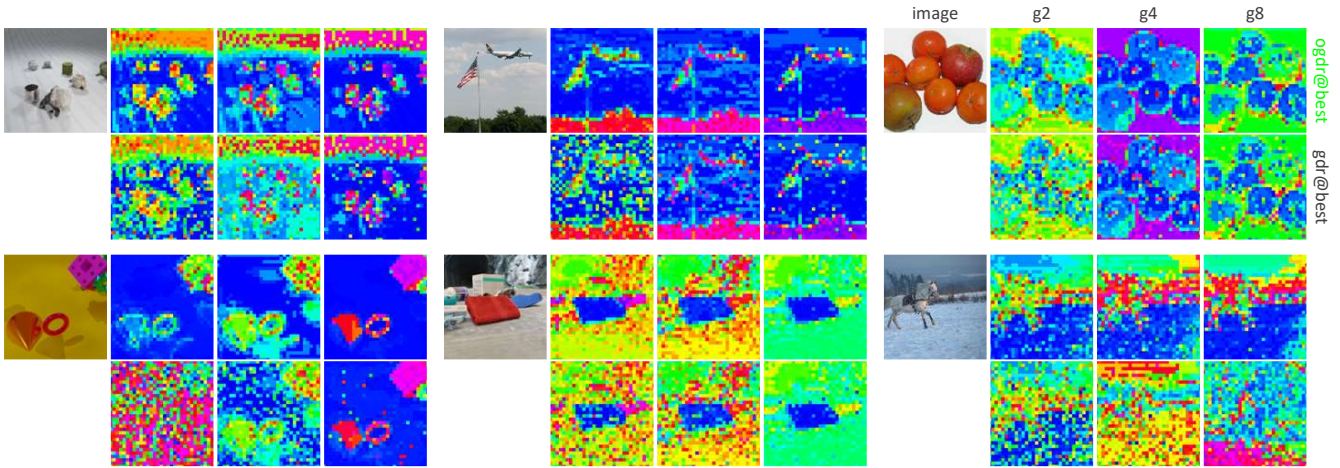


Figure 8: Object separability in VAE discrete representation by cosine similarity between superpixels and the central superpixel. Similar colors mean bigger similarity. Under group numbers 2/4/8, **OGDR** eliminates more pixel redundancy and preserves more object consistency thus provides clearer guidance to object representation learning than GDR does.

pansion rate contribute less to grouping channels belonging to the same attribute together. By contrast, high expansion rate is important for the diffusion-based, because the intermediate channel dimension is only 4, much less than that of the transformer-based, which is 256.

Pseudo-inverse of W as the *project-up* vs specified weights formulated in Eq. 8. We use specified weights as the project-up rather than using the pseudo-inverse of the project-down, but this mostly does harm to the performance. This again proves our design really organizes the channels for attribute decomposed grouping.

Using annealing *residual connection* formulated in Eq. 9 is always beneficial than not.

Normalization at last formulated in Eq. 11 is usually beneficial for diffusion-based OCL methods, but it has no obvious effect on transformer-based methods.

Conclusion

We propose organized grouped discrete representation technique to guide Object-Centric Learning better. Our technique outperforms the naive grouped discrete representation technique, and is applicable to both transformer-based OCL methods and diffusion-based ones. By statistical and visual analysis, we show that our organizing design truly facilitates channel grouping as decomposition from features to attributes, thus improving model expressivity and object representation learning guidance. Similar to GDR, there are some issues in our technique, like lower code utilization along with more groups and more hyper-parameters to tune in pretraining. These may be solved by borrowing ideas from VAE-related researches, which are left for future work.

References

Bahdanau, D.; Cho, K. H.; and Bengio, Y. 2015. Neural Machine Translation by Jointly Learning to Align and Translate. *International Conference on Learning Representations*.

| vqvae+ogdr@ $g4$ | expansion rate | | | |
|------------------|----------------|--------------------------------------|--------------------------------|--------------------------------|
| | 8c | 4c | 2c | 1c |
| c256-clevrtex | 0.0078 | 0.0075 | 0.0083 | 0.0079 |
| c256-coco | 0.0187 | 0.0191 | 0.0194 | 0.0192 |
| c4-clevrtex | 0.0102 | 0.0114 | 0.0132 | 0.0151 |
| c4-coco | 0.0233 | 0.0241 | 0.0261 | 0.0298 |
| vqvae+ogdr@ $g4$ | best setting | project-up pinv. \rightarrow spec. | residual w. \rightarrow w.o. | normaliz w. \rightarrow w.o. |
| c256-clevrtex | 0.0078 | 0.0081 | 0.0081 | 0.0079 |
| c256-coco | 0.0187 | 0.0188 | 0.0189 | 0.0188 |
| c4-clevrtex | 0.0102 | 0.0103 | 0.0132 | 0.0132 |
| c4-coco | 0.0233 | 0.0237 | 0.0317 | 0.0251 |

Table 1: Ablation studies measured by pretraining VAE reconstruction MSE. “c256” means VAE with intermediate channel dimension 256 for transformer-based methods and “c4” is 4 intermediate channels for diffusion-based ones; “g4” is that we use grouping number 4 as examples. “pinv. \rightarrow spec.” means the project-up with specified weights, rather than pseudo-inverse of the project-down. “w. \rightarrow w.o.” means removing the residual or normalization technique.

Bar, M. 2004. Visual Objects in Context. *Nature Reviews Neuroscience*, 5(8): 617–629.

Barnes, C.; Rizvi, S.; and Nasrabadi, N. 1996. Advances in Residual Vector Quantization: A Review. *IEEE Transactions on Image Processing*, 5(2): 226–262.

Burgess, C.; Matthey, L.; Watters, N.; et al. 2019. MONet: Unsupervised Scene Decomposition and Representation. *arXiv preprint arXiv:1901.11390*.

Caron, M.; Touvron, H.; Misra, I.; et al. 2021. Emerging Properties in Self-Supervised Vision Transformers. In *Proceedings of the IEEE/CVF International Conference on Computer Vision*, 9650–9660.

- Cavanagh, P. 2011. Visual Cognition. *Vision Research*, 51(13): 1538–1551.
- Chen, Y.; Fan, H.; Xu, B.; et al. 2019. Drop an Octave: Reducing Spatial Redundancy in Convolutional Neural Networks With Octave Convolution. In *Proceedings of the IEEE/CVF International Conference on Computer Vision*, 3435–3444.
- Elsayed, G.; Mahendran, A.; Van Steenkiste, S.; et al. 2022. SAVi++: Towards End-to-End Object-Centric Learning from Real-World Videos. *Advances in Neural Information Processing Systems*, 35: 28940–28954.
- Greff, K.; Kaufman, R. L.; Kabra, R.; et al. 2019. Multi-Object Representation Learning with Iterative Variational Inference. In *International Conference on Machine Learning*, 2424–2433. PMLR.
- Huang, G.; Liu, S.; Van der Maaten, L.; and Weinberger, K. 2018. CondenseNet: An Efficient DenseNet Using Learned Group Convolutions. In *Proceedings of the IEEE Conference on Computer Vision and Pattern Recognition*, 2752–2761.
- Jang, E.; Gu, S.; and Poole, B. 2017. Categorical Reparameterization with Gumbel-Softmax. *International Conference on Learning Representations*.
- Jiang, J.; Deng, F.; Singh, G.; and Ahn, S. 2023. Object-Centric Slot Diffusion. *Advances in Neural Information Processing Systems*.
- Kipf, T.; Elsayed, G.; Mahendran, A.; et al. 2022. Conditional Object-Centric Learning from Video. *International Conference on Learning Representations*.
- Krizhevsky, A.; Sutskever, I.; and Hinton, G. 2012. ImageNet Classification with Deep Convolutional Neural Networks. *Advances in Neural Information Processing Systems*, 25.
- Lim, K.-L.; Jiang, X.; and Yi, C. 2020. Deep Clustering with Variational Autoencoder. *IEEE Signal Processing Letters*, 27: 231–235.
- Locatello, F.; Weissenborn, D.; Unterthiner, T.; et al. 2020. Object-Centric Learning with Slot Attention. *Advances in Neural Information Processing Systems*, 33: 11525–11538.
- Oquab, M.; Darcet, T.; Moutakanni, T.; et al. 2023. DINOv2: Learning Robust Visual Features without Supervision. *Transactions on Machine Learning Research*.
- Palmeri, T.; and Gauthier, I. 2004. Visual Object Understanding. *Nature Reviews Neuroscience*, 5(4): 291–303.
- Rombach, R.; Blattmann, A.; Lorenz, D.; Esser, P.; and Ommer, B. 2022. High-Resolution Image Synthesis with Latent Diffusion Models. In *Proceedings of the IEEE/CVF Conference on Computer Vision and Pattern Recognition*, 10684–10695.
- Seitzer, M.; Horn, M.; Zadaianchuk, A.; et al. 2023. Bridging the Gap to Real-World Object-Centric Learning. *International Conference on Learning Representations*.
- Singh, G.; Deng, F.; and Ahn, S. 2022. Illiterate DALL-E Learns to Compose. *International Conference on Learning Representations*.
- Singh, G.; Kim, Y.; and Ahn, S. 2022. Neural Systematic Binder. *International Conference on Learning Representations*.
- Singh, G.; Wu, Y.-F.; and Ahn, S. 2022. Simple Unsupervised Object-Centric Learning for Complex and Naturalistic Videos. *Advances in Neural Information Processing Systems*, 35: 18181–18196.
- Van Den Oord, A.; Vinyals, O.; and Kavukcuoglu, K. 2017. Neural Discrete Representation Learning. *Advances in Neural Information Processing Systems*, 30.
- Vaswani, A.; Shazeer, N.; Parmar, N.; et al. 2017. Attention Is All You Need. *Advances in Neural Information Processing Systems*, 30.
- Watters, N.; Matthey, L.; Burgess, C.; and Alexander, L. 2019. Spatial Broadcast Decoder: A Simple Architecture for Disentangled Representations in VAEs. *ICLR 2019 Workshop LLD*.
- Wu, Z.; Dvornik, N.; Greff, K.; Kipf, T.; and Garg, A. 2023a. SlotFormer: Unsupervised Visual Dynamics Simulation with Object-Centric Models. *International Conference on Learning Representations*.
- Wu, Z.; Hu, J.; Lu, W.; Gilitschenski, I.; and Garg, A. 2023b. SlotDiffusion: Object-Centric Generative Modeling with Diffusion Models. *Advances in Neural Information Processing Systems*, 36: 50932–50958.
- Yang, D.; Liu, S.; Huang, R.; et al. 2023. Hifi-Codec: Group-Residual Vector Quantization for High Fidelity Audio Codec. *arXiv preprint arXiv:2305.02765*.
- Yi, K.; Gan, C.; Li, Y.; Kohli, P.; et al. 2020. CLEVRER: CoLlision Events for Video REpresentation and Reasoning. *International Conference on Learning Representations*.
- Zadaianchuk, A.; Seitzer, M.; and Martius, G. 2024. Object-Centric Learning for Real-World Videos by Predicting Temporal Feature Similarities. *Advances in Neural Information Processing Systems*, 36.
- Zhao, R.; Li, J.; and Wu, Z. 2022. Convolution of Convolution: Let Kernels Spatially Collaborate. In *Proceedings of the IEEE/CVF Conference on Computer Vision and Pattern Recognition*, 651–660.
- Zhao, R.; Wang, V.; Kannala, J.; and Pajarinen, J. 2024. Grouped Discrete Representation Guides Object-Centric Learning. *arXiv preprint arXiv:2407.01726*.
- Zhao, R.; Wu, Z.; and Zhang, Q. 2021. Learnable Heterogeneous Convolution: Learning both Topology and Strength. *Neural Networks*, 141: 270–280.

More Visualization

Here we supplement some visualization results that can not be put into the main text due to page limits. They are more about providing intuitive interpretability by visualization on our channel organizing and grouping.

Code Indexes

With our organized channel grouping as decomposition from features to attributes, we have attribute-level code indexes representing the intermediate representation. Thus like GDR “Grouped Discrete Representation Guides Object-Centric Learning” (Zhao et al., arXiv 2024), we can assign different colors to different indexes and then visualize it.

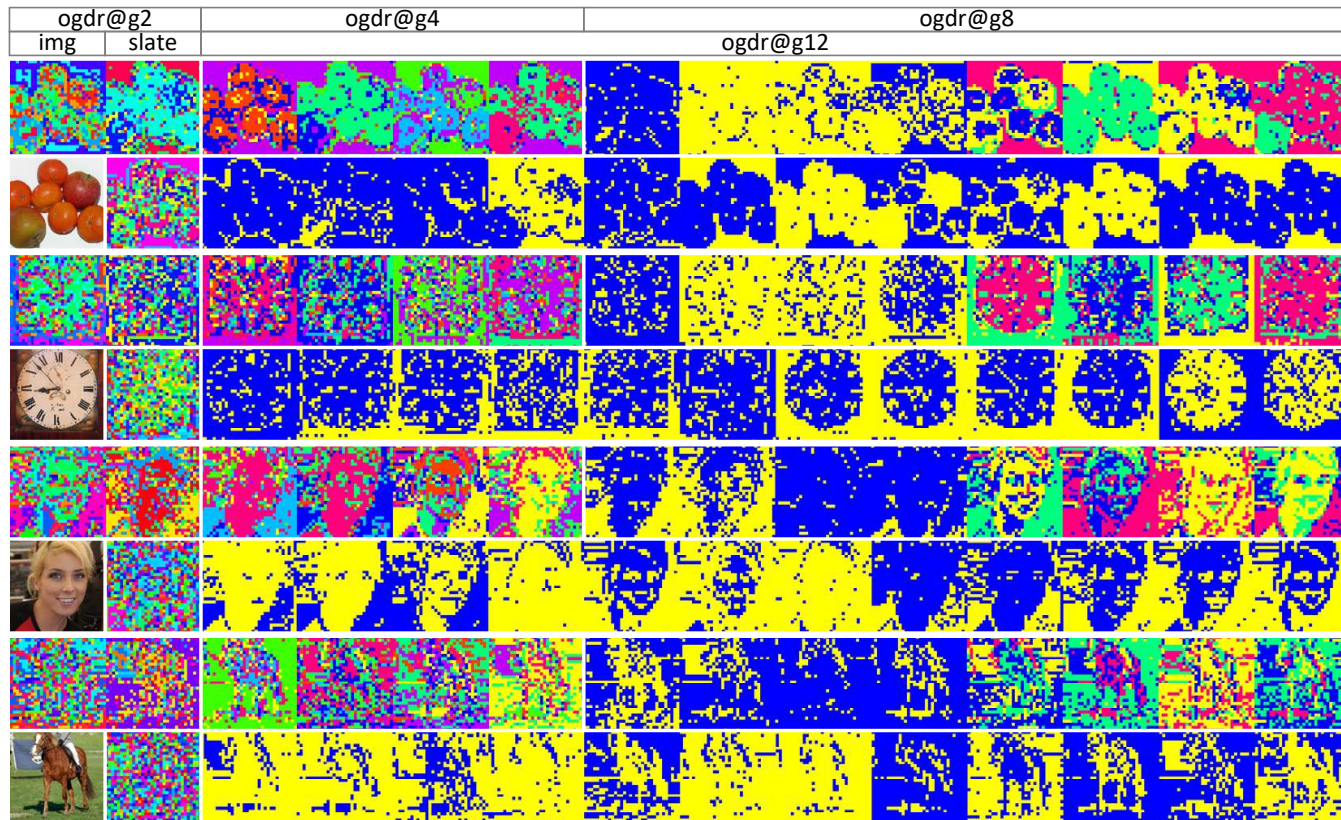


Figure 9: Visualization of OGDR intermediate representation in code indexes. “ogdr” is our OGDR technique, and “slate” is the non-grouped baseline. g_2 , 4, 8 and 12 are different grouping settings. Images are from COCO and VOC.

As we can see, our OGDR’s code indexes of different groups can extract different attributes in the image, like edges, textures, zones, colors and so on. By contrast, the non-grouped code indexes usually mix all of these together thus providing less guidance to object representation learning. That is one of the reasons our OGDR can boost existing transformer-based classics and diffusion-based state-of-the-arts.

Roughly, the more groups we use, the clearer discrete representation we have about different attributes. But according to the experiments in the main text, the OCL performance may not raise as accordingly. This can be attributed to the limited code utilization due to grouping, which is the same as that of GDR. This is a limitation of both GDR and our OGDR.

Channel Organizing

We argue that our project-up and projec-down design does organizing the intermediate representation channels so as to put channels belonging to the same attributes together for the following grouped discretization. We visualize this by drawing the project-up and project-down matrix weights in Sankey diagrams. For better visualization, we normalize the weights along both the input and output dimensions using softmax respectively.

As we can see, some of the input channels are mixed, switched or split into different attribute groups to discretization, and then the roughly inverse operation recover them to rebuild the input continuous representation in the form of discrete representation. We can see such clear projection patterns in most of the datasets and grouping numbers.

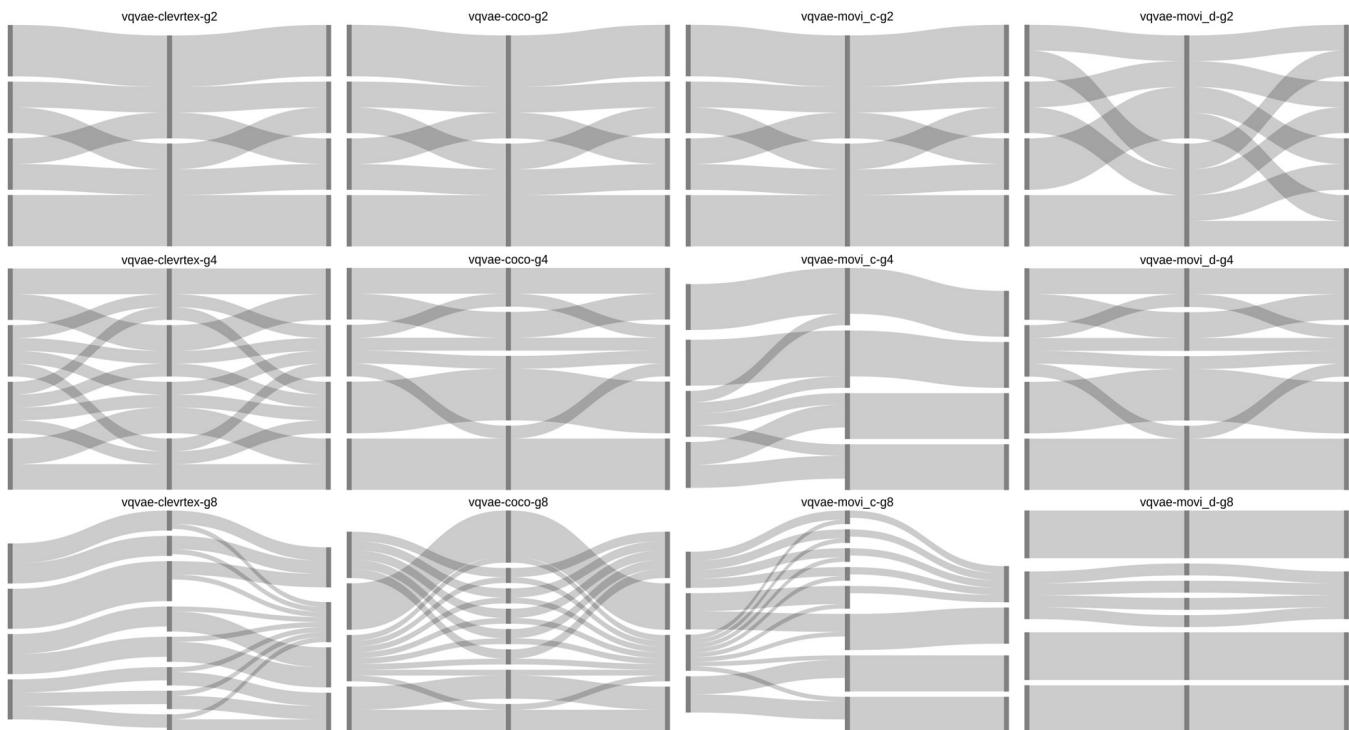


Figure 10: Visualization of OGDR project-up and project-down weights for channel organizing. Every sub plot has three columns of nodes (dark bars) and matrix weights among them (grey ribbons). Take “vqvae-clevrtex-g2” as an example. The first column of nodes correspond to the four channels of the continuous intermediate representation, the third column is discrete intermediate representation, and the second column two nodes are the two attribute groups to decompose from features to attributes.

Model Architecture

The overall architecture is drawn in Fig. 2. There are primary encoder, SlotAttention, transformer decoder or diffusion decoder, VAE encoder, codebook, and VAE decoder.

Primary Encoder

We use two kinds of primary encoder, which are unified for all experiments that have this module.

One is a naive CNN. This was first used in “Conditional Object-Centric Learning from Video” (Kipf et al., ICLR 2022) and then popularized as default setting in OCL models. We make a little modification. The modified architecture is $\{\text{conv}(k5s1p2)\text{-groupnorm}(32)\text{-mish}()\} * 4\}$ for short, which are in simple feed-forward without skip connections.

The other is DINO variant. The DINO is version 1, tiny, with downsampling rate 8, which was proposed in “Emerging Properties in Self-Supervised Vision Transformers” (Caron et al., ICCV 2021). We wrap it in big-little architecture by paralleling DINO with the aforementioned naive CNN, and then project plus upsample the output of DINO and sum it element-wisely with the output of naive CNN. The architecture is $\{\text{dino}()\text{-conv}(k3s1p1)\text{-upsample}(k8) + \text{naivecnn}()\}$ for short. Note that we freeze the weights of DINO because this preserves the foundational pretraining information in it leaving the naive CNN focus on adapting it with high spatial details, thus achieves better OCL performance.

Therefore, there is no spatial downsampling through this module.

SlotAttention

We follow the typical design of “Object-Centric Learning with Slot Attention” (Locatello et al., NeurIPS 2020). This is unified for all experiments that have this module.

Transformer Decoder

This is part of transformer-based methods like SLATE and STEVE.

We follow the typical design of “Illiterate DALL-E Learns to Compose” (Singh et al., ICLR 2022). This is unified for all experiments that have this module.

This decoder module operates on VAE intermediate representation/feature tensors with 4x4 spatial downsampling with respect to the input, by taking slots given by SlotAttention as the condition.
The input channel dimension of this module is 256.

Diffusion Decoder

This is part of diffusion-based methods like SlotDiffusion.

We follow the typical design of “SlotDiffusion: Object-Centric Generative Modeling with Diffusion Models” (Wu et al., NeurIPS 2023). This is unified for all experiments that have this module.

This decoder module operates on VAE intermediate representation/feature tensors with 4x4 spatial downsampling with respect to the input, by taking slots given by SlotAttention as the condition.

The input channel dimension of this module is 4.

VAE Encoder & Decoder

We follow the typical design of “Illiterate DALL-E Learns to Compose” (Singh et al., ICLR 2022). This is unified for all experiments that have this module.

There is spatial downsampling of 4x4 through VAE encoder and spatial upsampling of 4x4 through VAE decoder.

Codebook

This module is the one that differentiates between dVAE and VQ-VAE. And this is part of transformer-based and diffusion-based methods, respectively.

For the non-grouped codebook design, we follow the typical design of dVAE and VQ-VAE codebook in “Illiterate DALL-E Learns to Compose” (Singh et al., ICLR 2022) and “SlotDiffusion: Object-Centric Generative Modeling with Diffusion Models” (Wu et al., NeurIPS 2023), respectively.

For the grouped codebook design of SLATE/STEVE, we follow the original design of GDR proposed in “Grouped Discrete Representation Guides Object-Centric Learning” (Zhao et al., arXiv 2024). The organized grouped codebook design of SLATE, STEVE and SlotDiffusion is detailed in the main content of this paper.

The codebook module operates on VAE intermediate representation/feature tensors with 4x4 spatial downsampling with respect to the input.

There are 4096 codes in the non-grouped codebook, and of course 4096 attribute-combined codes in the grouped codebook. For transformer-based classics, the code dimension, i.e., VAE intermediate channel dimension, is 256; for diffusion-based state-of-the-arts, the code dimension is 4.

SLATE/STEVE

We mostly follow their original design for transformer-based classics, SLATE and STEVE, with their primary encoder, SlotAttention, decoder and VAE following the corresponding designs mentioned above. SLATE is for image OCL tasks. STEVE is a temporal version of SLATE for video OCL tasks, with an extra transformer encoder block to connect between current and next queries.

SlotDiffusion

We mostly follow its original design for diffusion-based state-of-the-arts, SlotDiffusion, with their primary encoder, SlotAttention, decoder and VAE following the corresponding designs mentioned above. We also designed its temporal version for video OCL tasks, by simply adding an extra transformer encoder block to connect from current to next queries.

DINOSAUR

This foundational-based OCL method, DINOSAUR, is only included as an reference. We follow its original work, but unify its primary encoder and SlotAttention to be the ones described above. This is only tested on COCO and VOC datasets.

SysBinder

This is an improver to the SlotAttention module of SLATE/STEVE. We follow its original design, with the remaining modules following the corresponding designs described above. We use the grouping number four as the unified setting across different experiments that have this module.

GDR

This is an improver to the VAE codebook module. We follow its original design, with the remaining modules following the corresponding designs described above.

We use grouping number two, four and eight, which are values that can exactly factorize the value 4096. Given 4096 codes in the codebook, the number of attributes in all attribute groups would be [64, 64], [8, 8, 8, 8] and [2, 2, 2, 2, 4, 4, 4, 4], respectively. Why these numbers? Simply because $64 \times 64 = 8 \times 8 \times 8 \times 8 = 2 \times 2 \times 2 \times 2 \times 4 \times 4 \times 4 \times 4 = 4096$, namely, we want to make fair comparison by controlling the same number of (attribute combined) codes.

OGDR

Our OGDR is detailed in the main text. The differences are as follows compared with GDR.

We use grouping number two, four, eight and twelve, which can exactly factorize the value 4096. We include g_{12} to evaluate the extreme effects of grouping cases. The corresponding attribute numbers in all attribute groups are [64, 64], [8, 8, 8, 8], [2, 2, 2, 4, 4, 4, 4] and [2, 2, 2, 2, 2, 2, 2, 2, 2, 2, 2, 2], respectively.

We use channel expansion rate 8 for both transformer-based classics and diffusion-based state-of-the-arts.

We use the final normalization for the diffusion-based state-of-the-arts, while not for the transformer-based classics.

Dataset Processing

The datasets for image OCL are ClevrTex, ClevrTex-OOD, COCO and VOC, where the latter two are real-world. The datasets for video OCL are MOVi-B, C, D and E, which are all synthetic. For different datasets, we have mostly the same processing but a bit differences.

Shared Preprocessing

To accelerate experiments, we adopt the dataset conversion scheme: Convert all datasets into LMDB database format, and load it into NVMe disk or RAM disk to minimize I/O overhead and maximize throughput.

Specifically, all images or video frames are center-cropped and re-sampled into 128x128, as well as their segmentation masks, and then are stored data type uint8 to save space. For images or videos, we use default interpolation mode; but for segmentation masks, we use NEAREST-EXACT interpolation mode.

During training, for both images and videos, we use spatial resolution of 128x128 as inputs and outputs. We normalize the input images or videos by minus 127.5 and divide 127.5, so that all elements are between -1 and 1. For videos, we also using random strided temporal cropping of fixed window size 6 to accelerate training and improve generalization.

During testing, there is no difference to that of training for images. But for videos, we need to remove the random strided temporal cropping and use the full video of 24 time steps.

ClevrTex & ClevrTex-OOD

The latter, ClevrTex-OOD, is an out-of-distribution version of the former, ClevrTex. Thus we only train on ClevrTex, and then evaluate on both.

As there are 10 objects at most in each image, we use number of slots queries of 10 + 1, where 1 represents for the background.

COCO & VOC

Both Microsoft COCO and Pascal VOC are real world datasets. We use the panoptic segmentation annotations of COCO, because OCL prefers panoptic segmentation rather than instance segmentation or semantic segmentation. But we have to use the semantic segmentation annotations of VOC because there are neither panoptic segmentation nor instance segmentation annotations available.

There can be lots of objects in an image, and there can be very small objects in an image. Considering the spatial resolution of 128x128, we filter out images that have more than 10 objects or have too small objects that are smaller than 16 bounding box area.

Accordingly, there are 10 things (plus stuff for COCO) at most in each image, we use the number of slots queries of 11.

MOVi-B/C/D/E

There are abundant annotations like depth, optical-flow, camera intrinsic/extrinsic parameters and so on. But for simple comparison, we only utilize the segmentation masks. We also keep the bounding box annotations of all objects in all time steps, because such conditioned query initialization is important and well-adopted in video OCL.

As there are 10, 10, 20 and 23 objects in these dataset, we use number of slots queries of 10+1, 10+1, 20+1, and 23+1, respectively.

Training Scheme

Following the convention, there are two training stages. The pretraining stage is for training VAE modules on corresponding datasets, so as to learn good discrete intermediate representation. The OCL training stage, which utilize the pretraining VAE representation as guidance for object centric learning.

Pretrain VAE

For all datasets, we use total number of training iterations 30,000, and validation interval iterations 600, so that we have about 50 checkpoints for every OCL model on every dataset. But to save storage, we save only the latter half 25 checkpoints. This is unified across all datasets.

The batch size for image datasets is 64, while for video datasets it is 16. This holds for both training and validation. This setting is shared across all datasets.

For multi-process, we use the number of workers 4. This holds for both training and validation. This setting is shared across all datasets.

For the non-grouped dVAE, the objective is the MSE formulated in SLATE/STEVE. For group-dVAE, i.e., GDR, the objectives are MSE and utilization loss formulated in GDR “Grouped Discrete Representation Guides Object-Centric Learning” (Zhao et al., arXiv 2024).

For non-grouped VQ-VAE, the objectives are MSE, align and commit losses formulated in “Neural Discrete Representation Learning” (van den Oord et al., NeurIPS 2017). But for grouped VQ-VAE, the objectives are MSE, align and commit losses, plus the aforementioned utilization loss.

We use Adam optimizer with initial learning rate of $2e-3$. And the learning rate is manipulated by cosine annealing scheduling, with a linear warmup during first 1/20 of total steps. This setting is shared across all datasets.

We use automatic mixed precision provided by PyTorch autocast API. Along with this, we use PyTorch builtin gradient scaler, so as to apply gradient clipping of maximum norm 1.0. This setting is shared across all datasets.

For GDR and OGDR, to balance the exploration and exploitation, we manipulate the τ value for VAE’s Gumbel sampling if there is. It starts from 10 at training start and keeps constant until half of the total steps, and then changes to 0.1 in the latter half of the total steps. During validation or testing, this value is of course not valid as we use argmax instead of Gumbel sampling.

Initialize Slots Queries

The query initializer is used to provide initial value for aggregating dense feature map of the input into slots that represent different objects and the background.

For image datasets, i.e., ClevrTex, COCO, VOC, we use random query initialization. Such an initialization is learning a set of Gaussian distributions and then sample samples from them. Here we have two parameters: One is the means of the learnt Gaussian distributions, and it is a set of trainable parameters, which is of dimension c ; Another is the shared sigma (scale value) of the learnt Gaussian distributions, and it is not trainable, instead, it is manipulated under a cosine annealing scheduling and is fixed to 0 during evaluation. These two set of parameters are of the same dimension size as the slots queries.

For video datasets, i.e., MOVi-B/C/D/E, we use another way for initialization. This is projecting the prior information about objects and the background, e.g., bounding boxes, into a set of vectors: Firstly, Bounding boxes are normalized by dividing them with the height and width of the input image or video frame, and then flattened into a set of 4-dimensional vector, whose number is the number of slots; Afterwards, they are processed by a two-layer MLP, with GELU as the intermediate activation, to project them into the channel dimension of c , the same as the slots.

Train OCL Model

For all datasets, we use total number of training iterations 5,0000, and validation interval iterations 1000, so that we have about 50 checkpoints for every OCL model on every dataset. But to save storage, we only save the latter half of the total checkpoints. This setting is shared across all datasets.

The batch size for image datasets is 32 for both training and validation, while for video datasets it is 8 for training and 4 for validation as there are more time steps in videos during validation. This setting is shared across all datasets.

For multi-process, we use the number of workers 4. This holds for both training and validation. This setting is shared across all datasets.

The objective is the CE loss between the predicted image/video token classes and the discrete intermediate representation of input image/video, as formulated in SLATE/STEVE papers.

Metrics used here are ARI, mIoU and mBO, calculating the panoptic segmentation accuracy of both objects and the background. This setting is shared across all datasets.

We use Adam optimizer with initial learning rate of $2e-4$. And the learning rate is manipulated by cosine annealing scheduling, with a linear warmup during first 1/20 of total steps. This setting is shared across all datasets.

We use auto mixed precision provided by PyTorch autocast API. Along with this, we use PyTorch builtin gradient scaler, so as to apply gradient clipping of maximum norm 1.0 for images and 0.02 for videos.

For random query initialization, we manipulate the σ value of the learned non-shared Gaussian distribution to balance the exploration and exploitation. On multi-object datasets, it starts from 1 at training start and decays to 0 at training end under cosine annealing scheduling; but on single-object datasets, it remains 0 from beginning to the end. During validation or testing, this value is set to 0, eliminating any uncertainty for best performance.

Remember we load the pretrained weights of VAE modules to guide the OCL model. For SLATE/STEVE and SLATE/STEVE+SysBinder, we load weights of dVAE and GDR (grouped dVAE); For SLATE/STEVE+OGDR, we load

weights of VQ-VAE+OGDR (grouped VQ-VAE) under corresponding group numbers; For SlotDiffusion(+OGDR), we load weights of VQ-VAE(+OGDR). For DINOSAUR, we follow that of the original paper.